Supplementary Material

File S1. Lithology and chronology of the Rybnaya and Ulukh-Chayakh sequences.

The lithological composition of the Rybnaya Mire comprises sandy clay between 400-344 cm (8.5-7.0 ka) with peat from 344 cm to the top of the profile (7-0 ka). At Ulukh-Chayakh Mire sandy clay accumulated between 348-310 cm and gyttja between 310 and 300 cm (>6.0 ka), followed by peat from 300 cm to the surface of the profile (<6.0-0 ka). The chronology of both cores was established based on AMS radiocarbon measurements performed on both plant macrofossils and bulk material at Isotoptech, Debrecen, Hungary (Table S1). The ^{14}C AMS age estimates were converted to calendar years BP using the IntCal20 data set of Reimer et al. (2020) and the age-depth models were constructed using a smooth spline method implemented by CLAM software (Blaauw, 2010). In the age-depth models, an age of -67 cal yr BP (coring year 2017 at Rybnaya) and -69 cal yr BP (coring year 2019 at Ulukh-Chayakh) was assigned to the surface samples of each sequence. Both sites show an inversion of some of the radiocarbon measurements. Although plant macrofossils are preferred over bulk material for radiocarbon dating, bulk peat has been shown to yield reliable age information at sites in both Europe and western Siberia (Holmquist et al., 2016). However, larger differences were observed between dates on bulk peat and wood (see details in Holmquist et al., 2016). The radiocarbon measurements on plant remains yielded slightly more inconsistent ages, as opposed to those on bulk peat that were in a consistent chronological order. For example, the younger age of the wood piece (4815 ^{14}C at 390 cm) embedded in the sandy clay, in the bottom sequence of Rybnaya, as compared to measurements above (6727 ^{14}C at 364 cm and 4742 ^{14}C at 340 cm) suggested that this was probably a wood fragment dragged down from an upper layer during coring, or may reflect ex situ material such a tree remains relocated by flooding and buried. At Ulukh-Chayakh, the radiocarbon age inversion of 2331±37 at 185 cm (Rosaceae seeds), as compared to the measurements above (2808±26 at 144 cm on peat) corresponds to Ti high values (Table S1; Fig S5). This age inversion may reflect the influence of flood events occurring on the adjacent Chulym River between 4 and 3 ka. This period was marked by high flooding activity, which could have inundated the terrace above the floodplain where this mire is located (Leshchinskiy et al., 2011). In the age-depth models, we retained those radiocarbon measurements which produced age-depths with the lowest number of age reversals (Fig. S1). The age-depth model of the Rybnaya sequence shows a mean peat accumulation rate of 25 yr/cm (ranging 6-36 yr/cm). The Ulukh-Chayakh sequence covered ~ the last 8500 years, but the chronology of the bottom part of this site (>6000 years) was based on linear extrapolation and is therefore highly speculative (Fig. S2). The section of the sequence covering the last 6000 years had a mean temporal resolution of 21 yr/cm (ranging between 3-37 yr/cm).

Table S1. Radiocarbon dates of the Rybnaya and Ulukh-Chayakh sequences.

Lab code	**Depth (cm)**	**^{14}C age (yr BP)**	**Material dated**
Rybnaya			
DeA-20877	45	Modern (post 1950)	*Sphagnum*
DeA-23650	60	61±34	Bulk peat
DeA-20878	145	2898±30	*Sphagnum* stems
DeA-23651	160	3016±37	Bulk peat
DeA-23652	220	4209±41	Bulk peat
DeA-20879	245	4424±32	*Sphagnum* stems
DeA-20880	295	5067±37	*Sphagnum* stems
DeA-23653	320	5480±42	Bulk peat
DeA-20881	340	4742±45	*Sphagnum* stems
DeA-23654	364	6728±50	Gyttja
DeA-20882	390	4815±34	Wood
Ulukh-Chayakh			
DeA-25837	27	Modern (post-1950)	Bulk peat
DeA-23655	45	550±35	Cyperaceae seeds
DeA-25838	90	1043±23	Bulk peat
DeA-23656	135	2710±37	Cyperaceae & Rosaceae seeds
DeA-25839	144	2808±26	Bulk peat
DeA-20878	185	2331±37	Rosaceae seeds
DeA-25840	215	3447±27	Bulk peat
DeA-23658	265	4702±40	Rosaceae seeds, Wood, Ericaceae leaves
DeA-25841	283	5275±34	Bulk peat
DeA-23659	311	3703±41	Organic Matter (unidentified)

Fig S1. Age depth models of the Rybnaya (a) and Ulukh-Chayakh (b) sequences.

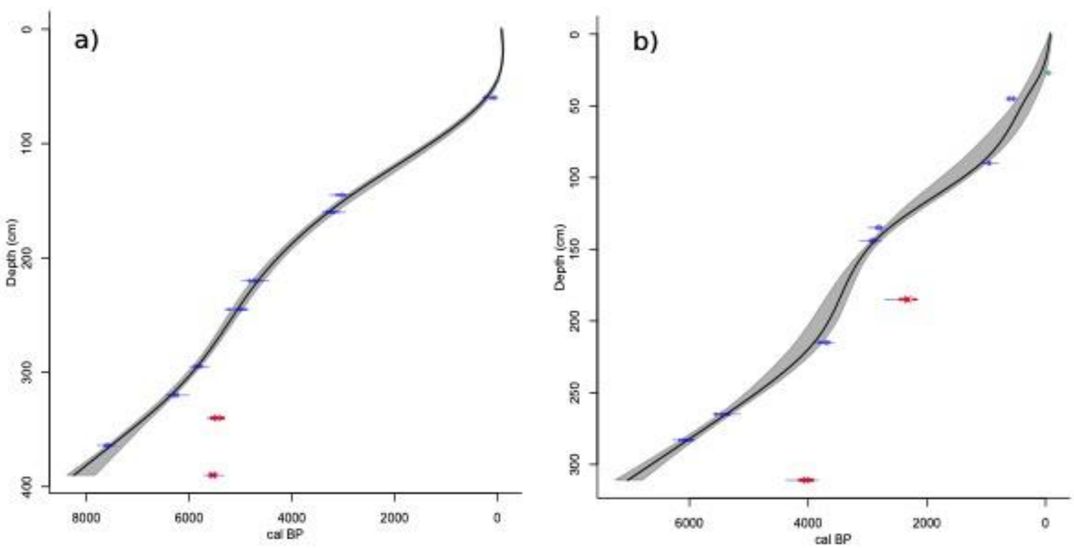

Fig S2. Deposition time (cm / yr) of the Rybnaya (a) and Ulukh-Chayakh sequences.

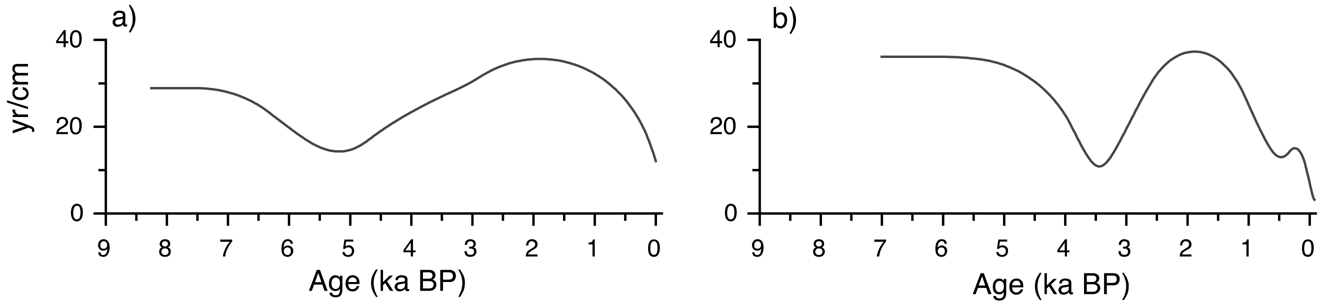

File S2. Charcoal-based reconstructions of fire history

We estimated the frequency and severity of fire episodes from charcoal peaks extracted from the macrocharcoal influx (CHAR>150 µm) using CharAnalysis software (Higuera et al., 2009). We first decomposed the total CHAR component into CHAR background (Cbackground) and CHAR-peaks (Cpeak) reflecting local fire episodes. The CHAR time series were first interpolated to constant time steps (Cinterpolated) of 30 yr at both sites. To identify the time interval or window width that maximises the signal-to-noise ratio we used a robust Lowess smoother with several window widths (e.g., 200, 300, 600, 700 and 900 yr). A Gaussian mixture model with a locally defined threshold was used to distinguish noise-related variations from local charcoal peaks. Charcoal values exceeding the 95th percentile threshold of the modelled noise distribution were identified as potential fire episodes and the fire episode frequencies were smoothed to the same window width used to determine Cbackground. We incorporated the cut-off probability for minimum count analysis to further screen and remove insignificant charcoal peaks. Evaluation of CHAR outputs including goodness of fit (GOF) and signal-to-noise index (SNI) showed that for an interpolated window width of 30 yr and a smoothing window width of 900 yr (30 yr *30 samples), the SNI was well above three at both sites (Higuera et al., 2009; 2011; Kelly et al., 2011). Therefore, we chose to use this setting for both sites (Figs. S3a, S3b). Fire frequency (FF) at each site was determined based on the total number of fires within a 900-yr time window by counting the number of charcoal peaks within that window. The charcoal peak extraction approach was designed for systems with high severity stand-replacing fires (Higuera et al., 2009), whereas fires in the study area are dominated by surface fires with an infrequent occurrence of stand-replacing fires. The high values of signal-to-noise ratio suggest that this method is suitable for charcoal peaks extractions and reliably indicates the occurrence of high-severity local fires (FigS2a,b).

Fig S2a. Peak sensitivity analysis at Rybanya (acronym SK). a) Decomposition of interpolated CHAR component into CHAR background and CHAR peaks. Dotts above crosses suggest peaks that passed the sensitivy test, i.e., charcoal values exceeding the 95th percentile threshold; b) Changes in mean fire return interval (FRI) by using alternative theresholds; c) Local signal-to-noise index, where values above 3 indicate the theoretical minimum value for justification of peak extraction; d) Global signal-to-noise index average the values of the entire sequence.

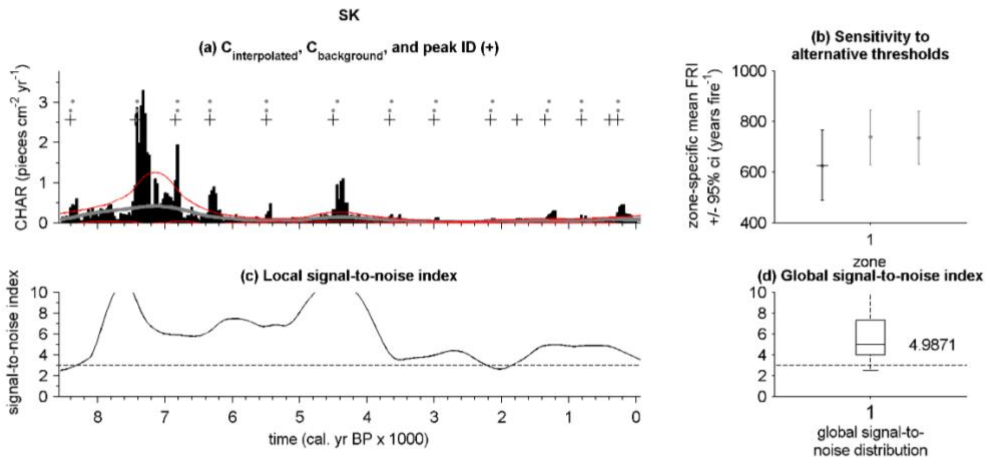

Fig S2b. Peak sensitivity analysis at Ulukh Chayakh (acronym ST). For interpreation of individual pannels see above.

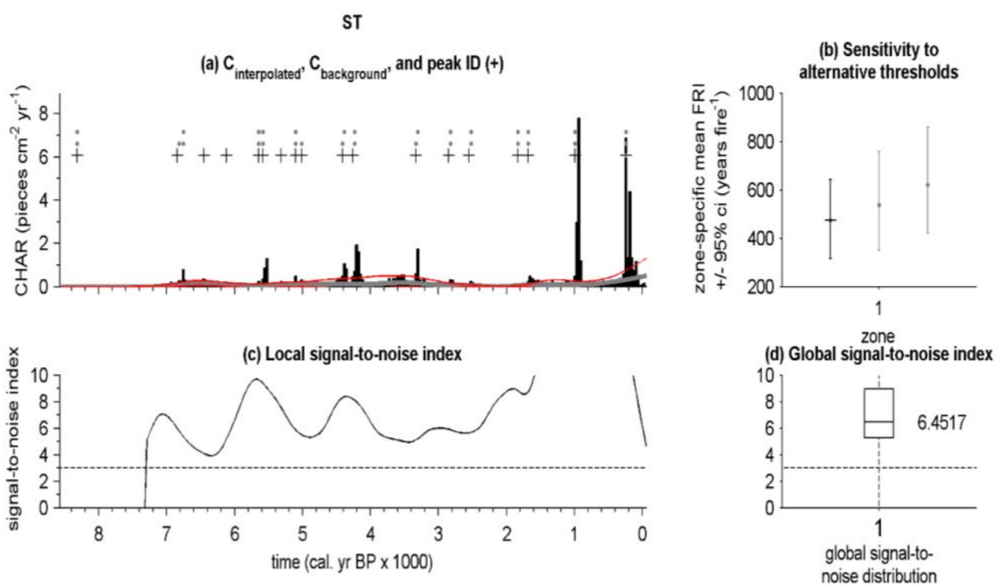

File S3a. Macrocharcoal influx separated into morphologies for the two sequences. Additionally, length to with ratio (*L:W*) and charcoal surface area (μm^2) were measured on selected samples in Ulukh-Chayakh sequence only.

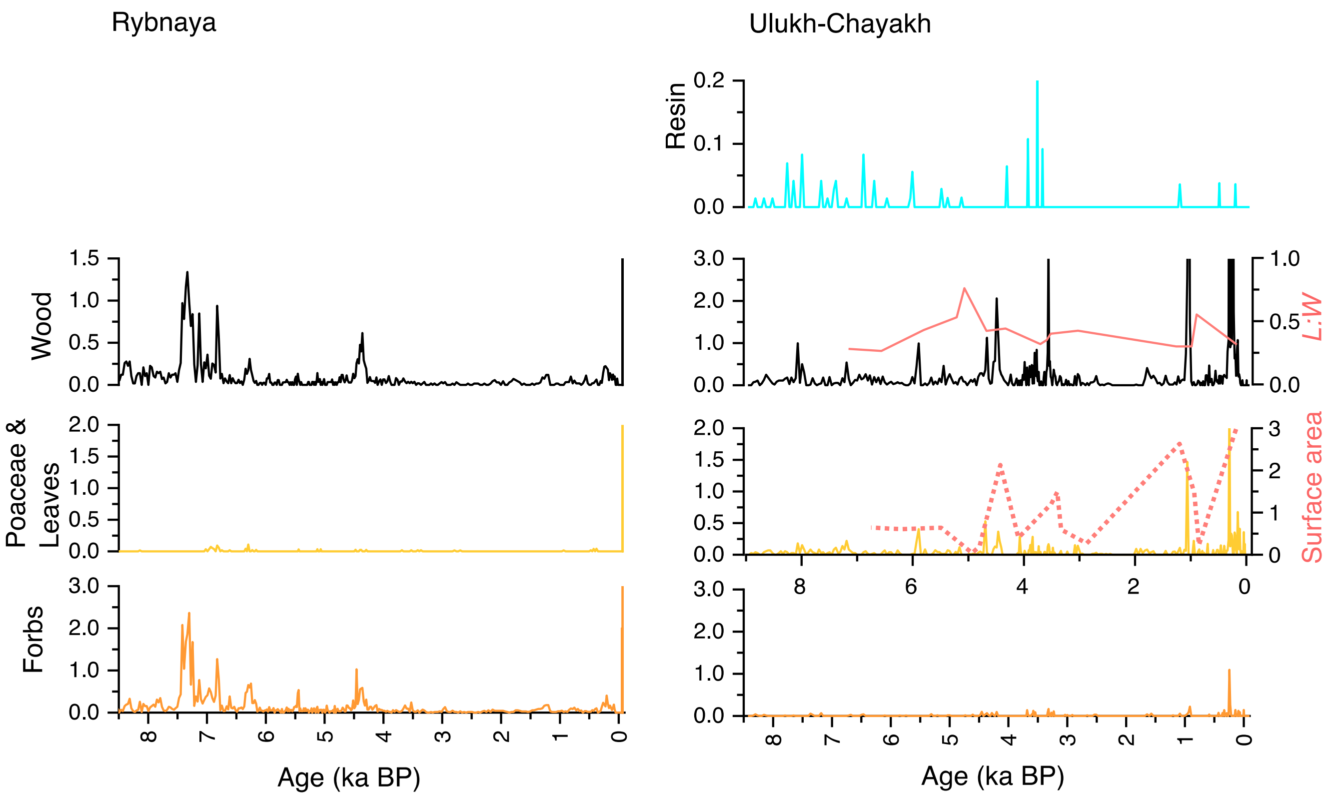

File S3b. Macrocharcoal influx (particles >150 µm / cm^{-2} yr^{-1}) separated into the four size classes as well as microcharcoal influx in the Rybnaya and Ulukh-Chayakh sequences.

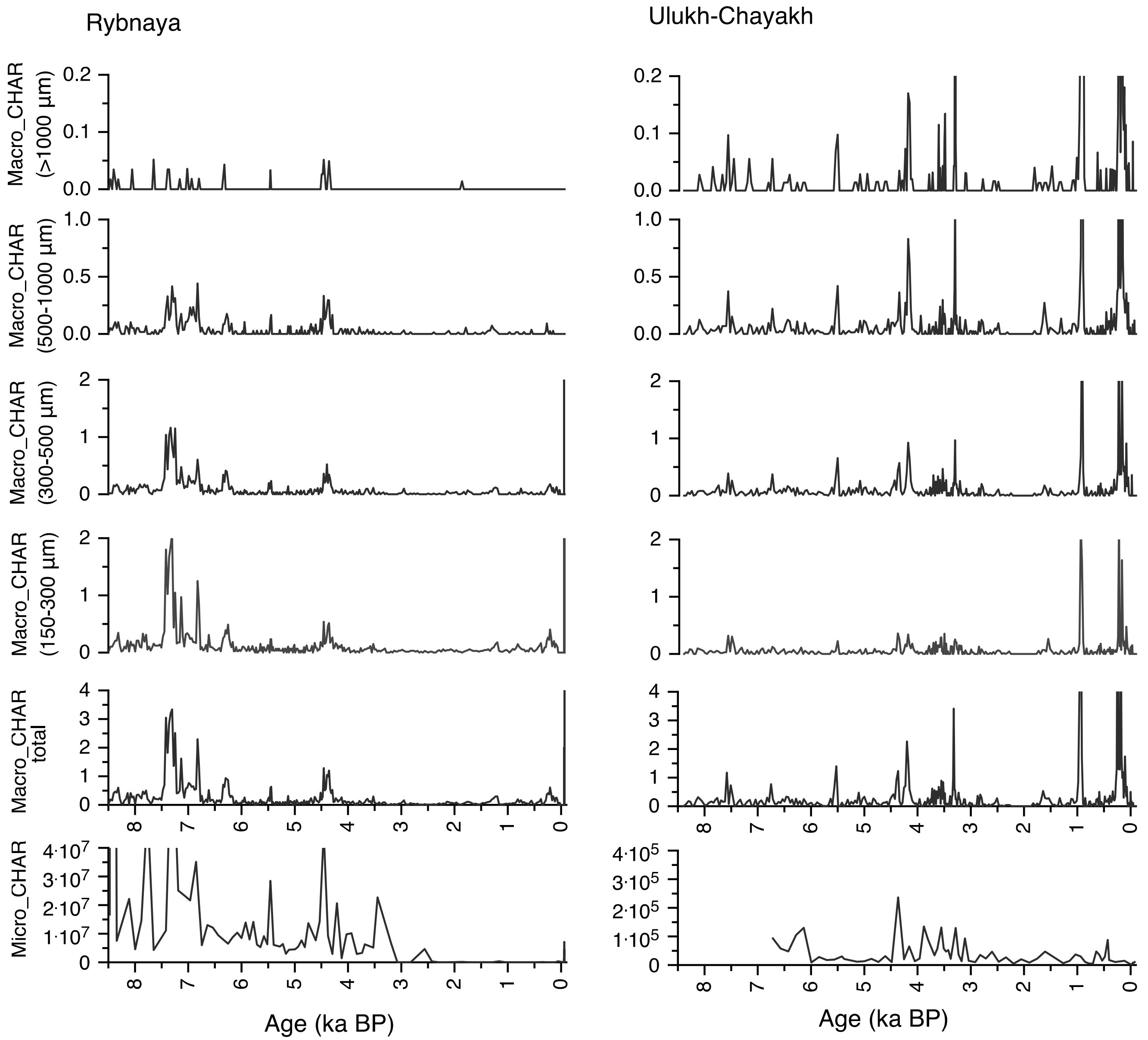

File S4a. Pollen diagram of the Rybnaya sequence.

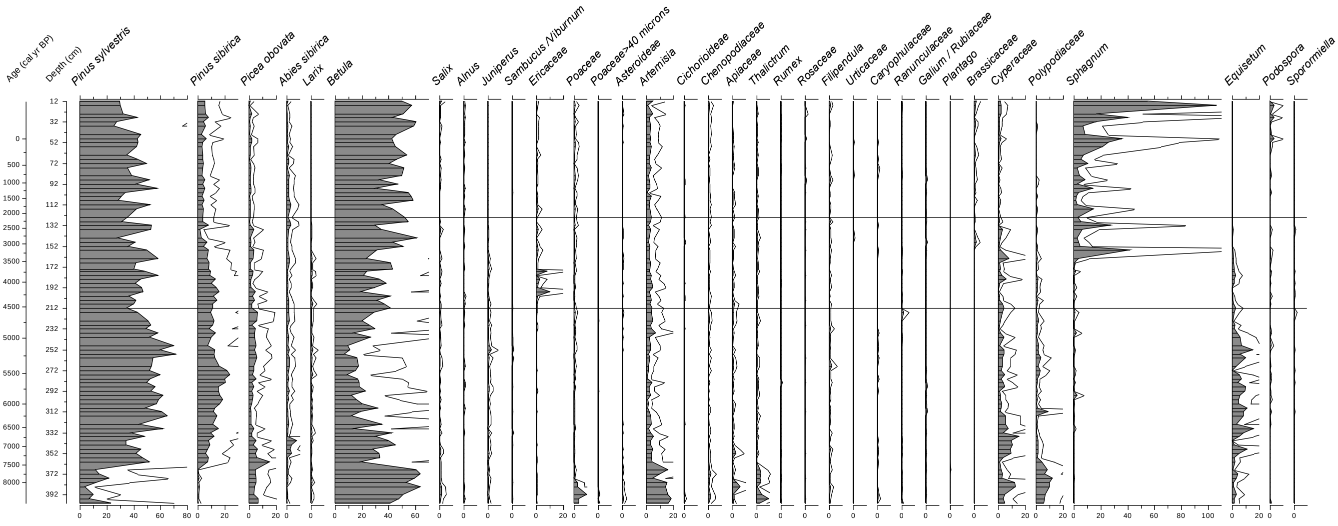

File S4a. Pollen diagram of the Ulukh-Chayakh sequence.

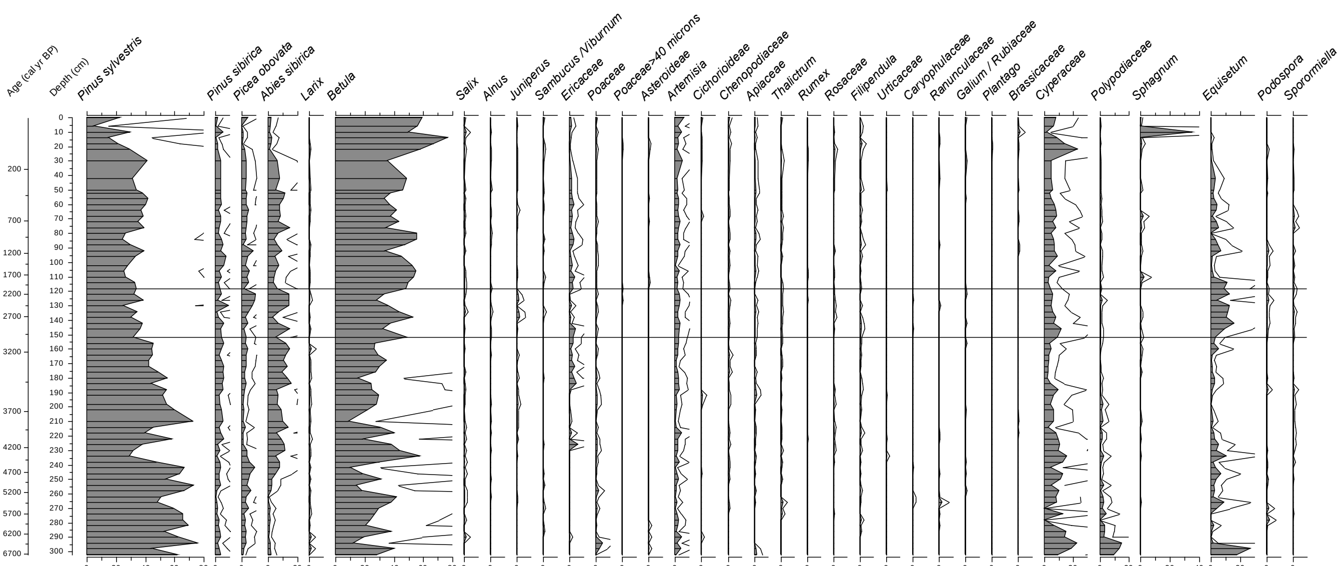

File S5. Geochemical element Ti, versus DTW (presented as Z-scores) at Rybnaya (a) and Ulukh-Chayakh

As a lithogenic (or geogenic) indicator Ti can be seen as an indicator of detrital input reflecting the mineralogical content, as opposed to the highly organic nature of peat profiles. The source of this material will reflect both the type of mire and the events leading to this input. In an ombrotrophic context, the input will be entirely aeolian. Here the landscape position of the site means that at the mire stage, a fluvial input is feasible as a transport mechanism for the delivery of such material and associated lithogenic signal. We therefore interpret the higher Ti content in the basal, minerogenic portion pre-dating the peat onset at Rybnaya and Ulukh-Chayakh as reflecting the minerogenic substrate at the sites. We refer to subsequent Ti fluctuations as indicating possible flood events. The increased fluvial input between 4 and 3 ka, likely reflect flooding or channel position change as a transport mechanism for the delivery of such material (File S5), an interpretation supported by the intensification in flood activity during this time period (Leshchinskiy et al., 2011).

Fig S5 Geochemical element Ti, versus DTW (presented as Z-score) at Rybnaya (a) and Ulukh-Chayakh (b).

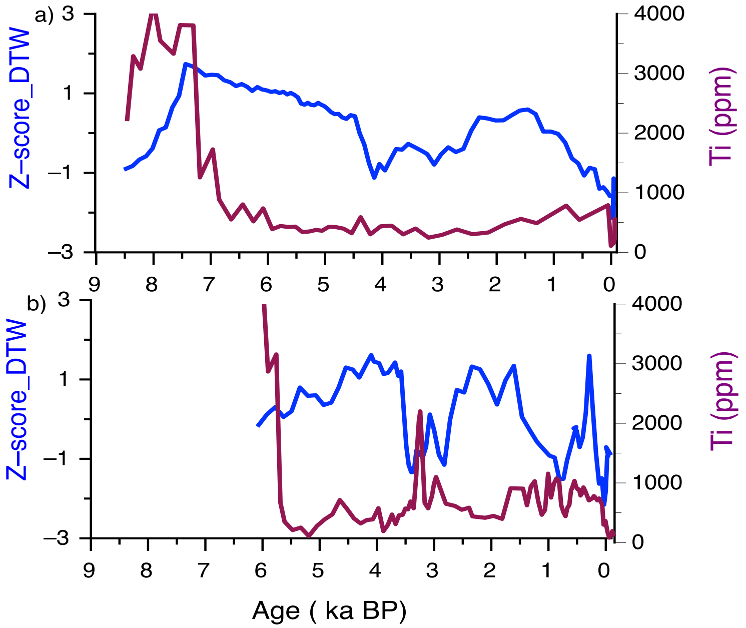

References

Blaauw, M.: Methods and code for ‘classical’ age-modelling of radiocarbon sequences. Quaternary Geochronology 5, 512–518, https://doi.org/10.1016/j.quageo.2010.01.002, 2010.

Higuera, P., Brubaker, L., Anderson, P., Hu, F., and Brown, T.: Vegetation mediated the impacts of postglacial climate change on fire regimes in the south-central Brooks Range, Alaska. Ecological Monographs 79, 201-219, https://doi.org/10.1890/07-2019.12009, 2009.

Kelly, R.F, Chipman, M.L., Higuera, P.E., Stefanova, I., Brubaker, L.B., and Hu, F.S.: Recent burning of boreal forests exceeds fire regime limits of the past 10,000 years. Proceedings of the National Academy of Sciences, 110, 13055-13060, https://doi.org/10.1073/pnas.1305069110, 2013.

Leshchinskiy, S. V., Blyakharchuk, T.A., Vvedenskaya, I.A., Orlova, L.A.: The first terrace above the Ob’floodplain near Kolpashevo: the age and formation conditions." Russian Geology and Geophysics 52.6, 641-649, 10.1016/j.rgg.2011.05.007, 2011.

Holmquist, J.R., Finkelstein, S.A., Garneau, M., Massa, C., Yu, Z., MacDonald, G.M.: A comparison of radiocarbon ages derived from bulk peat and selected plant macrofossils in basal peat cores from circum-arctic peatlands. Quaternary Geochronology, 31, 53-61. https://doi.org/10.1016/j.quageo.2015.10.003, 2016.

Higuera, P.E., Gavin, D.G., Bartlein, P.J., Hallett, D.J.: Peak detection in sediment charcoal records: impacts of alternative data analysis methods on fire history interpretations. Int. J. Wildland Fire 19, 996e10145, 2011.

Reimer, P., Austin, W., Bard, E., Bayliss, A., Blackwell, P., Bronk Ramsey, C., . . . Talamo, S.: The IntCal20 Northern Hemisphere Radiocarbon Age Calibration Curve (0–55 cal kBP). Radiocarbon, 62, 725-757. doi:10.1017/RDC.2020.41, 2020.